The 27th Iranian Conference on Optics and Photonics (ICOP 2021), and the 13th Iranian Conference on Photonics Engineering and Technology (ICPET 2021). University of Sistan and Baluchestan, Zahedan, Iran, Feb. 2-4, 2021

کد مقاله : ۲-۲۱۱۳-۱۰-A

# جاذب کامل پلاسمونی مبتنی بر ساختار فلز-عایق- فلز بعنوان یک حسگر با حساسیت بالا

**زهرا مددی**

**دانشکده مهندسی برق و کامپیوتر، دانشگاه آزاد اسلامی، واحد علوم و تحقیقات،تهران، ایران**

**چکیده- در این مقاله، یک ساختار نانومقیاس فلز- عایق- فلز با دو طراحی متفاوت نانومنفذ متقارن در لایه فلز بالایی به عنوان یک حسگر جاذب کامل پیشنهاد شده است. طیف جذب ساختار با استفاده از روش عددی تفاضل محدود - حوزه زمان سه بعدی برای تابش عمود پرتو نور موج صفحه‌ای در محدوده‌ی طول موج ۱۸۰۰ تا ۲۳۰۰ نانومتر محاسبه گردیده است. به منظور حسگری ضریب شکست محلول‌های گلوکز، آنالیت مذکور درون منافذ ساختار ریخته می‌شود. طبق نتایج شبیه سازی، یک پیک تشدید در طیف جذب مشاهده شده، که با افزایش ضریب شکست آنالیت به سمت طول موج‌های بالاتر جابجا می‌گردد. حساسیت و حد تشخیص حسگر به ترتیب202.22 nm/RIU و0.0131 برای طراحی نانومنفذ اول، و 328.19 nm/RIU و 0.0126 برای طراحی نانومنفذ دوم به دست آمده است. از این رو، هر دو ساختار پیشنهادی با طراحی‌های متفاوت نانومنفذهای تناوبی برای حسگری مایعات مختلف با ضرایب شکست نزدیک به هم بسیار مناسب می‌باشند.**

**کلید واژه-** حسگر جاذب کامل، ضریب شکست، فلز- عایق- فلز، منافذ متقارن.

# Metal-Insulator-Metal based Plasmonic Perfect Absorber as a High-Sensitivity Sensor

**Zahra Madadi**

**Department of Electrical and Computer Engineering, Science and Research Branch, Islamic Azad University, Tehran, Iran .**

**Abstract-** In this paper, a nanoscale Metal-Insulator-Metal (MIM) structure with two different nano-aperture designs in the upper metal layer is proposed as a Perfect Absorber Sensor (PAS). The absorption spectrum of the structure is calculated using the 3D FDTD numerical method for the perpendicular incidence of a plane wave light within 1800-2300 nm wavelength range. In order to sense the refractive index of glucose solutions, these analytes are poured into the apertures of the structure. Simulation results show that a resonance peak is obtained in the absorption spectrum which is red-shifted with increasing the refractive index of the analyte. The sensitivity and detection limit were obtained 202.22 nm/RIU and 0.0131 for the first design, and 328.19 nm/RIU and 0.0126 for the second design, respectively. Hence, both structure designs are very suitable for different liquids sensing with refractive indices close to each other.

Keywords: Metal-Insulator-Metal, Perfect Absorber Sensor, Refractive Index, Symmetrical Apertures;

## 1. Introduction

In recent years, the metal-insulation-metal (MIM) structures have emerged as one of the most common plasmonic perfect absorber designs. These technologies have been developed towards achieving a narrower perfect absorption band for sensor applications. In MIM absorber devices, the upper layer usually consists of periodic metal nano-apertures or nano-particles array, which separated by a layer of insulator from a flat metal layer at the bottom

of the structure. The bottom metal layer will be designed as a continuous metal sheet with a thickness higher than the penetration depth of incident wavelengths; and, it acts as a perfect reflector mirror.The localized surface plasmon resonances (LSPRs) are excited at the interface of the upper metal layer and the insulator layer. The use of LSPRs provided by sub-wavelength metal structures is a promising trick to achieve perfect light absorption in specific frequency bands [1,2]. Currently, many researchers are working on the modeling and construction of perfect absorber sensors based on tiny windows in the upper metal layer. Because in such structures, good contact is made between the analyte fluids and the sensor surface [3,4]. In this paper, we design a nanoscale Au-$MgF_2$-Au structure with two different nano-aperture arrays in the upper gold layer as a perfect absorber sensor. A spacer layer of magnesium fluoride insulation is placed on this gold mirror and on top of that, the third layer of the structure with a periodic array of apertures is perched. For the sensing process, analyte fluids are poured into the apertures. The article is organized as follows, in section 2, the structure design of the proposed sensor is described. In section 3, the simulation results of two aperture designs are compared based on sensitivity and Figure of Merit (FOM). In section 4, the research conclusion is presented.

## 2. Structure Design

The MIM unit cell of perfect absorber sensor structure with two different aperture designs in its upper metal layer for pouring analytes (water-soluble glucose) into it is shown in Fig. 1. In this structure, there is a gold layer with an infinite array of apertures at the top, and a gold mirror at the bottom, which are separated by a $MgF_2$ insulator layer.

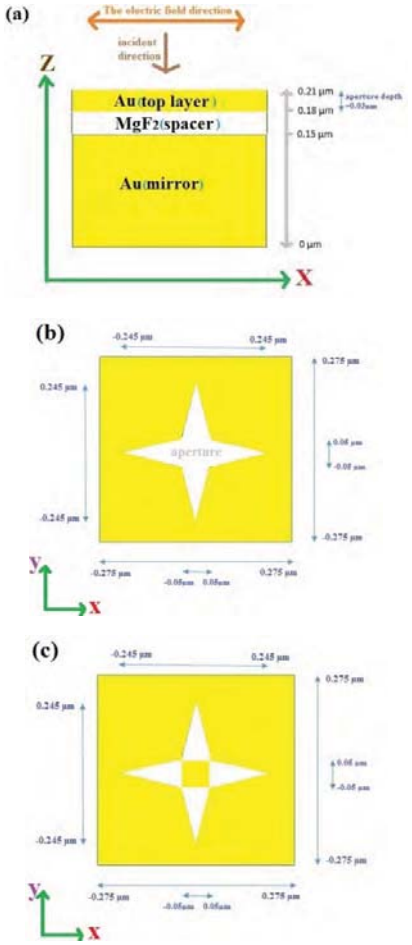


Fig. 1: The absorber unit cell: (a) 2D side view of the structure on the z-x plane, The 2D top view of the structure for(b)aperture design 1,(c)aperture design 2.

The thickness of the bottom, middle, and top layers in the direction of z are $t_1$ = 150 nm, $t_2$ = 30 nm, and $t_3$ = 30 nm, respectively. The depth of apertures in the upper gold layer is equal to $t_3$. Two different aperture designs are shown in Figures. 1(b) and 1(c). The unit cell periodicity in x and y directions are equal Px = Py =550 nm.

In structure simulation using the 3D Finite-Difference Time-Domain (FDTD) numerical method, the simulation environment is limited from the upward and downward directions in z to the boundary condition of the perfectly match layer (PML), and in the x and y directions are limited by the periodic boundary condition. A plane wave of light within 1.8-2.3 μm wavelength range is incited in z direction and perpendicular to the structure. The dielectric constant of gold in the near-infrared spectral range is described by the Drude model [5]. The refractive index of the $MgF_2$ is defined from Ref [6]. The Reflection (R) and Transmission (T) spectra of the absorber are obtained in the incident wavelength range and then the Absorption spectrum (A) is calculated from the relation A = 1-T-R. Note that the reflection spectrum is reflected power intensity of sensor structure, and the transmittance spectrum is completely suppressed by the bottom gold mirror (T=0)[7].

## 3. Simulation Results

In this step, analytes with different refractive indices are poured into the structure apertures. Then, the absorption spectra for each of them are measured and shown in Figure. 2. The resonance peak in the absorption spectrum shifts with changing analyte refractive index. The resonance wavelength curve versus the refractive index for both designs is shown in Figure 2(c). We can calculate the sensitivity (S) of the sensor using relation $S=\Delta\lambda_p/\Delta n$. Where $\Delta\lambda_p$ is the resonance peak shift, and $\Delta n$ is a refractive index unit (RIU) variations [8]. The sensitivity of the first and second aperture designs was obtained 202.22 nm/RIU, and 328.19 nm/RIU, respectively. In order to evaluate the sensor performance, the figure of merit and the limit of detection are calculated as FOM=S/FWHM and LOD=$(3\Delta\lambda_{un})/S$, respectively [9]. Where FWHM is the full width at half maximum of resonance peak and $\Delta\lambda_{un}$ is uncertainty in determining the peak position. The FOM and LOD were obtained 1.36 and 0.0131 for the first design, and 2.01 and 0.0126 for the second design, respectively.

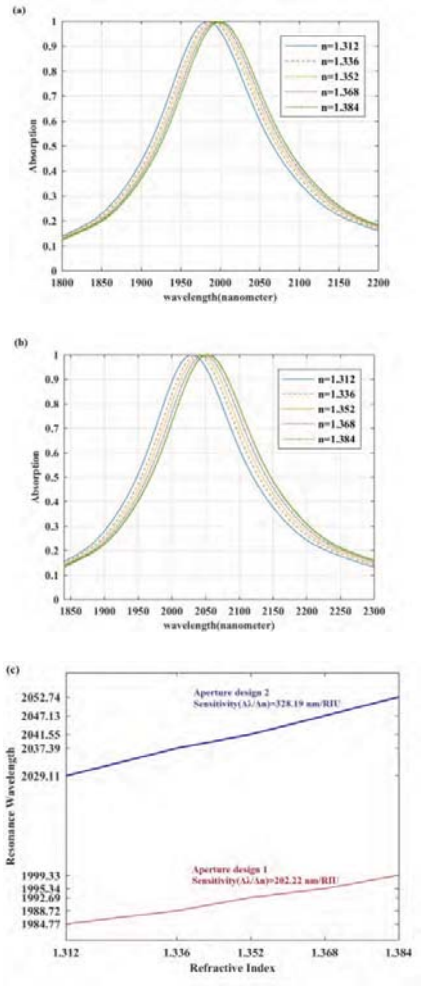


Fig. 2: The structure absorption spectrum for (a) aperture design 1,(b) aperture design 2, (c)The curve of the resonance wavelength versus refractive index.

In another step, a 2D field monitor with y-x cutting plane [-0.275μm ≤(x & y)≤ 0.275μm] inserted in the position of z=0.2μm. The analyte refractive index is considered n=1.312. Then, the absolute value of the electric field distribution (Abs(E)) at the resonant wavelength and in coordinate x = 0 μm on the y-axis is calculated. As shown in Figure. 3, the electric field distribution in both designs is mostly concentrated at the positions y = (+0.16 & -0.16) μm inside the apertures. In the second aperture design, due to the presence of central gold metal between the triangular apertures, the electric field coupling of the two apertures in positions y> 0 and y <0 is reduced, and therefore the FWHM is greater than the first design.

## 4. Conclusion

In this paper, a Perfect Absorber Sensor (PAS) based on a nanoscale Au-$MgF_2$-Au structure with two different symmetrical aperture designs in the upper gold layer has been presented. The resonance peak FWHM, Sensitivity(S) and FOM were obtained 148 nm, 202.22 nm/RIU, and 1.36, respectively, for the first aperture design, and for the second designer, 163 nm, 328.19 nm/RIU, and 2.01, respectively. It should be noted that these resonance peak sensitivities are obtained for both designs, make them very suitable for sensing the different liquids with a low refractive index difference.

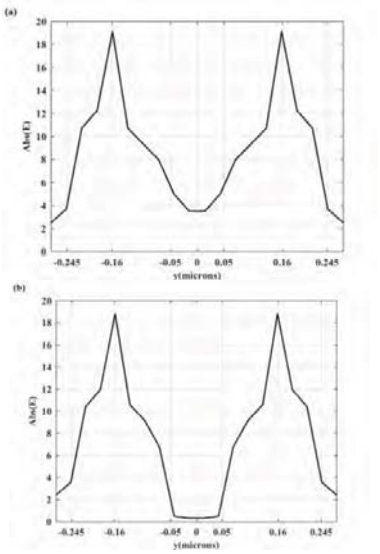


Fig. 3: Abs (E) at the resonant wavelength (1984.77 nm and 2029.11 nm for the first and second design, respectively) in coordinates z = 0.2 μm and x = 0 μm on the y axis for (a) aperture design 1, (b) aperture design 2.

## References

**[1]** C. Chen, G. Wang, Z. Zhang, "Dual narrow-band absorber based on metal-insulator-metal configuration for refractive index sensing", OPTICS LETTERS. **43**(15), 3630-3633, 2018.

**[2]** S. Luo, J. Zhao, D. Zuo, X. Wang, "Perfect narrow band absorber for sensing applications", OPTICS EXPRESS. **24**(9), 9288-9294, 2016.

**[3]** P. Mandal, "Plasmonic Perfect Absorber for Refractive Index Sensing and SERS", Plasmonics. **11**(1), 223-229, 2016.

**[4]** K. V. Sreekanth, M. Elkabbash, Y. Alapan, A. R. Rashed, U. A. Gurkan, G. Strangi, "A multiband perfect absorber based on hyperbolic metamaterials", Scientific Reports. **6** ,1-8, 26272, 2016.

**[5]** M. A. Ordal, L.L. Long, R. J. Bell, S. E. Bell, R. R. Bell, R. W. Alexander, C. A. Ward, "Optical properties of the metals Al, Co, Cu, Au, Fe, Pb, Ni, Pd, Pt, Ag, Ti, and W in the infrared and far infrared", Appl. Opt. **22**(7), 1099-1119, 1983.

**[6]** E. D. Palik, Handbook of Optical Constants of Solids Academic Press, 1998.

**[7]** F. Cheng, X. Yang, J. Gao, "Enhancing intensity and refractive index sensing capability with infrared plasmonic perfect absorbers", OPTICS LETTERS. **39**(11), 3185-3188, 2014.

**[8]** J. Hammond, N. Bhalla, S. Rafiee, "Localized Surface Plasmon Resonance as a Biosensing Platform for Developing Countries", Biosensors. 4, 172-188, 2014.

**[9]** L. Tong, H. Wei, S. Zhang, "Recent Advances in Plasmonic Sensors", Sensors. 14, 7959-7973, 2014.